Experimental Study on Influence of a Pile Penetration on Deformation of a Buried Pipe in Sand

Kensuke MORITA
Civil engineer, Sato Kogyo Co. Ltd., Tokyo, Japan
Tatsunori MATSUMOTO
Professor, Graduate School of Kanazawa University, Kanazawa, Japan
Email: matsumoto@se.kanazawa-u.ac.jp
Anh Tuan VU
Lecturer, Department of Civil Engineering, Le Quy Don Technical University, Hanoi, Vietnam

ABSTRACT

In this paper, influence of installation of new piles on an existing buried pipe was investigated through small-scale model tests. Close-ended aluminum pipes of 595 mm in length and 32.0 mm in outer diameter were used for the model piles in dry sand model ground. A close-ended PVC pipe of 700 mm in length and 18.0 mm in outer diameter was used as a buried pipe model. The PVC pipe was instrumented with axial strain gauges to obtain bending moments in vertical and horizontal directions. The PVC pipe was set in the model ground horizontally at a depth 230 mm. The model piles were pressed-in into the ground from the ground surface at locations near the buried pipe. The distributions of the buried pipe displacements in the vertical and horizontal directions were estimated using the measured bending moments. The experiments were carried out in dense (relative density D_r = 80%) and loose (D_r = 50%) sand grounds. The paper presents the experimental results, and discusses the influential factors, such as distance between the piles and the buried pipe, the pile tip level and soil density, on the deformation of the buried pipe.

Key words: *Buried pipe, Pile installation, Experiment, Deformation, Sand*

1. Introduction

Owing to recent developments of press-in or jack-in machines for piles and/or sheet piles, precise positioning of installed piles became possible and the construction machine is able to access the vicinity of existing superstructures or underground structures such as piles, underground walls and buried pipes. In Japanese pile design codes, it is prescribed that interaction (pile group effects) between two piles can be negligible if centre-to centre pile spacing, *s*, is greater than 2.5. The authors, however, have a doubt on this specification. Also, in case of installing a new pile in the vicinity of a buried pipe, influence of the newly installed pile on the buried pipe may not be negligible.

In this research, fundamental small-scale model tests were carried out to investigate how installation of new piles affects the behaviours of an existing pipe buried in dry sand model ground.

2. Experiment description

2.1. Model pile

Close-ended aluminum pipes having a length, L , of 595 mm, an outer diameter, D_o, of 32.0 mm and an inner diameter, D_i, of 29.3 mm were used for the model piles. The specifications of the model pile are listed in **Table 1**. Each model pile (P1, P2 and P3) was instrumented with strain gauges at 5 different levels, and the pile shaft was coated with sand particles to increase the shaft resistance, as shown in **Fig. 1.**

Table 1. Specifications of model pile

Pile length, L_p (mm)	595
Outer diameter, D_o (mm)	32
Inner diameter, D_i (mm)	29.3
Wall thickness, t_w (mm)	1.35
Density, ρ_p (g/cm^3)	2.70
Young's modulus, E_p (MPa)	65,400
Poisson's ratio, ν_p	0.33

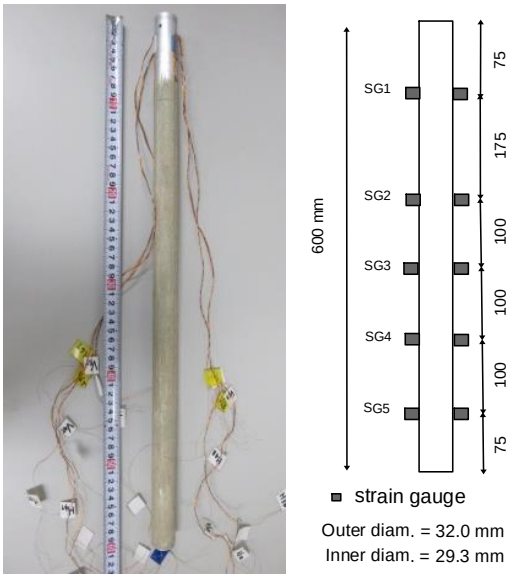

Fig. 1 Model pile instrumented with strain gauges

2.2. Model buried pipe

A PVC (PolyVinyl Chloride) pipe having L_{pipe} = 701 mm, $D_{o\ pipe}$ = 18.0 mm, $D_{i\ pipe}$ = 12.6 mm was used as a buried pipe. Both ends of the PVC pipe were closed (capped) to prevent intrusion of sand particles inside the pipe. The specifications of the PVC pipe are listed in **Table 2**. The pipe was instrumented with axial strain gauges at 7 sections (see **Fig. 2)**. At each measurement section, 4 strain gauges were glued on the pipe shaft 90 degrees apart, to obtain bending moments in vertical and horizontal directions.

2.3. Model ground

Dry silica sand #6 was used for model ground in the experiments. The physical properties of the sand are listed in **Table 3**.

A model ground was prepared in a rigid box having dimensions of 800 mm in length, 500 mm in width and 530 mm in depth.

Table 2. Specifications of model buried pipe

Length, L_{pipe} (mm)		701
Outer diameter, $D_{o\ pipe}$ (mm)		18.03
Inner diameter, $D_{i\ pipe}$(mm)		12.56
Cross-sectional area, A_{pipe} (mm^2)		131.4
Moment of inertia, I_{pipe} (mm^4)		3965.8
Position of strain gauges (Distance from pipe end, in mm)	1	50
	2	150
	3	250
	4	350
	5	450
	6	550
	7	650
Young's modulus, E_{pipe} (N/mm^2)		2705.3
Poisson's ratio, ν_{pipe}		0.407
Shear modulus, G_{pipe} (N/mm^2)		961.4

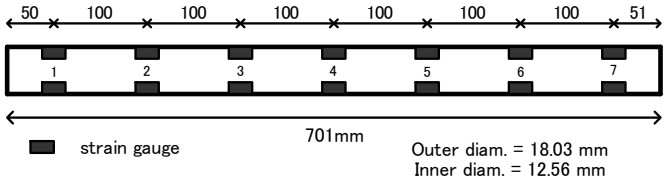

Fig. 2 Model buried pipe instrumented with strain gauges

Table 3. Physical properties of silica sand #6

Mean particle size, D_{50} (mm)	0.21
Soil particle density, ρ_s (ton/m^3)	2.67
Max. dry density, ρ_{dmax} (ton/m^3)	1.60
Min. dry density, ρ_{dmin} (ton/m^3)	1.27
Max. void ratio, e_{max}	1.10
Min. void ratio, e_{min}	0.66

The sand was poured in the soil box by about 50 mm thick and tamped to have prescribed relative density, D_r, of 80% (ρ_d = 1.53 t/m^3, called dense ground) or 50 % (ρ_d = 1.42 t/m^3, loose ground). The model pipe was set horizontally in the ground as shown in **Fig. 3** in the process of ground preparation. After the setting of the pipe, sand pouring and tapping were repeated until the total ground height reached 530 mm (10 layers of 50 mm in thickness and 1 layer of 30 mm in thickness).

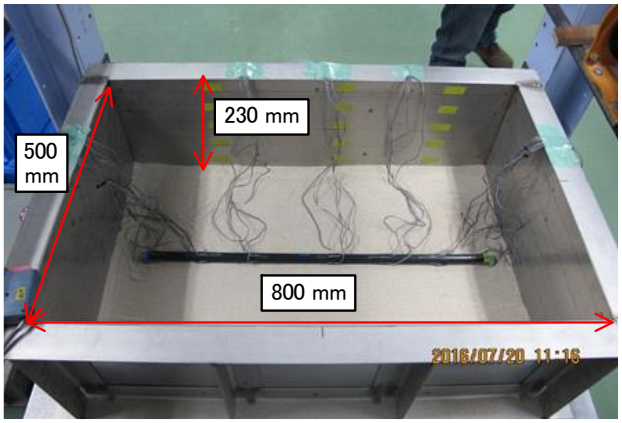

Fig. 3 Model ground and the buried pipe

Cone penetration tests (CPTs) were conducted in the model ground after the completion of experiments in each model ground. The diameter of the cone used was 20.5 mm which was smaller than that of the outer diameter of the model pile. **Fig. 4** shows the CPT results in the dense and loose model grounds. In both grounds, the tip resistance, q_t, increases almost linearly with depth, although q_t in the dense ground is about 5 times that in the loose ground.

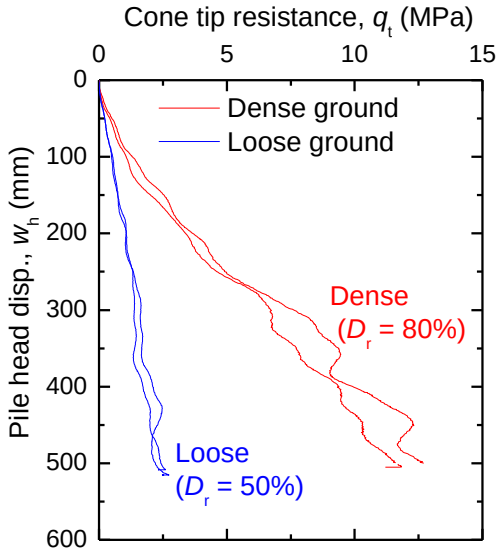

Fig. 4 CPT results in the dense and loose model grounds

2.4. Triaxial CD tests of the sand

In order to grasp the mechanical behaviours of the sand, a series of triaxial CD compression tests were carried out (Vu, 2017). For the dense sand (D_r = 80%), five CD tests were carried out with different confining pressures, p_0, of 7, 17, 27, 50 and 100 kPa. For the loose sand (D_r = 50%), a CD test with p_0 = 10.5 kPa was carried out. The results of the CD tests are shown **Fig. 5** and **Fig. 6**.

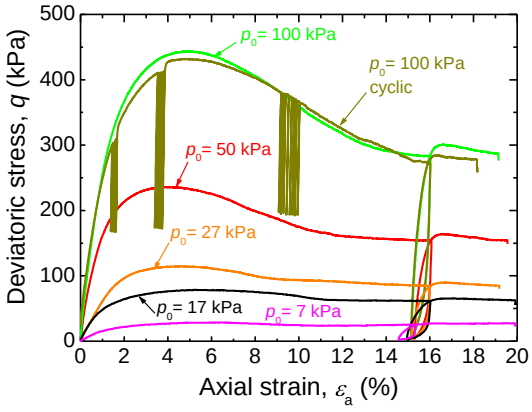

(a) Axial strain ε_a vs deviatoric stress q

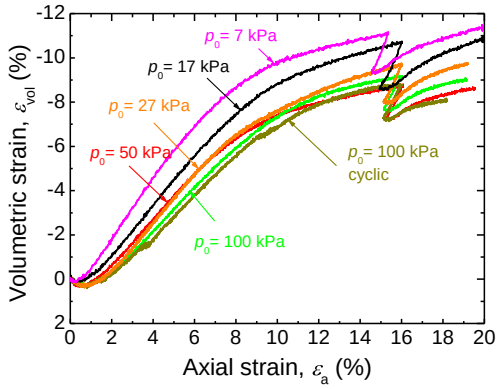

(b) Axial strain ε_a vs volumetric strain ε_{vol}

Fig. 5 Results of triaxial CD tests for the dense sand

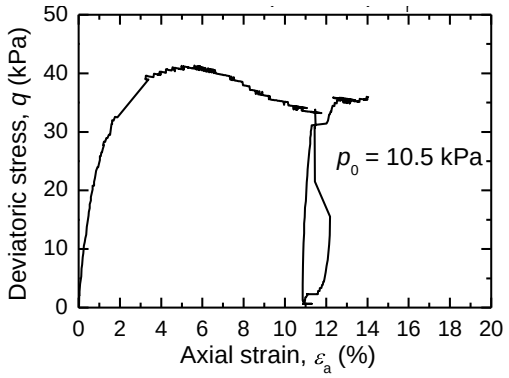

(a) Axial strain ε_a vs deviatoric stress q

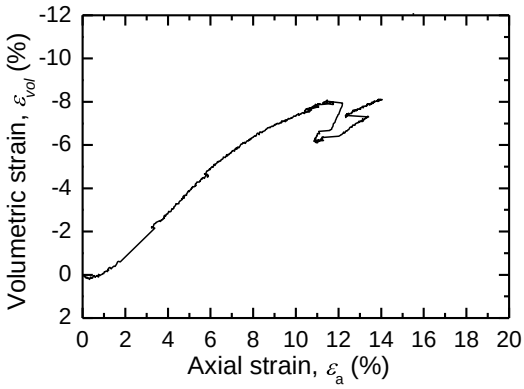

(b) Axial strain ε_a vs volumetric strain ε_{vol}

Fig. 6 Results of triaxial CD test for the loose sand

For the dense sand, the internal friction angle, ϕ_p', at peak peak strength is 42.8 degrees and the friction angle at residual state, ϕ_r', is 35 degrees. It is seen from **Fig. 5(a)** that the initial stiffness, $\Delta q/\Delta\varepsilon_a$, increases almost linearly with increase in the square root of p_0. It is seen from **Fig. 5(b)** that a small amount of negative dilatancy occurs at a very early stage of shearing followed by a large amount of positive dilatancy. Positive dilatancy behaviour weakens after the axial strain, ε_a, exceeds about 8%.

The results of the CD test of the loose sand show similar trend to those of the dense sand, although ϕ_p' and ϕ_r' of the loose sand is 38 degrees. It is seen from comparison of the dilatancy curve of the dense sand with p_0 = 7 kPa (**Fig. 5(b)**) and that of the loose sand with p_0 = 10.5 kPa (**Fig. 6(b)**) that degree of positive dilatancy is reduced in the loose sand.

2.5. Test procedure

The same test procedure was used basically in the experiments in the dense and the loose grounds. The PVC pipe was buried in the model ground horizontally at a depth of 230 mm, as shown in **Fig. 3** (the depth is defined as the depth of the axis of the PVC pipe). Thereafter, the model pile P1 was pressed into the ground first quasi-statically at a penetration speed of 0.2 mm/s until the pile tip level reached about 400 mm depth. Then, the pile P2 was pressed into the ground similarly, and finally the pile P3 was installed. The locations in plan of P1, P2 and P3 in the case of the dense sand are shown in **Fig. 7(a)**. For an example, the horizontal distance between the axis of P1 and the shaft of the PVC buried pipe was 64 mm. Note that in the case of the loose sand, the horizontal distance between P1 and the PVC pipe was 85 mm although 64 mm was intended.

3. Experimental results

3.1. Penetration resistance of piles in the dense and loose grounds

Fig. 8 shows the pile head load, P_h, (penetration resistance) with the pile head displacement (almost equal to the pile tip depth), w_h, measured in the cases of the dense and the loose grounds. In the case of the dense sand, P_h is larger in the piles pushed-in later, especially for depths greater than 250 mm. Penetration of P1 would have displaced the soils surrounding the pile, resulting in higher stresses and higher density of the surrounding soils. P2 was pushed into the influenced soils. Hence, it is reasonable that P2 has higher P_h and that P3 is subjected to more influence from the previously installed piles P1 and P2.

The pile head load, P_h, of P1 in the loose ground is much lower than that in the dense ground, as expected from the CPT results in both grounds (**Fig. 4**).

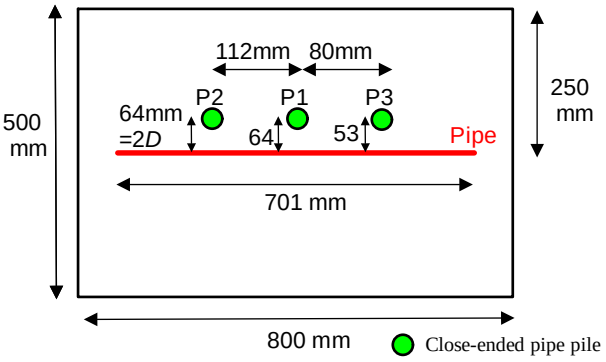

(a) Top view

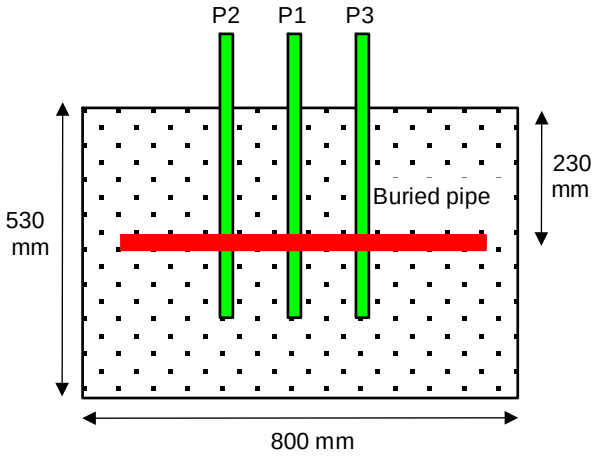

(b) Side view

Fig. 7 Locations of the buried pipe and the piles

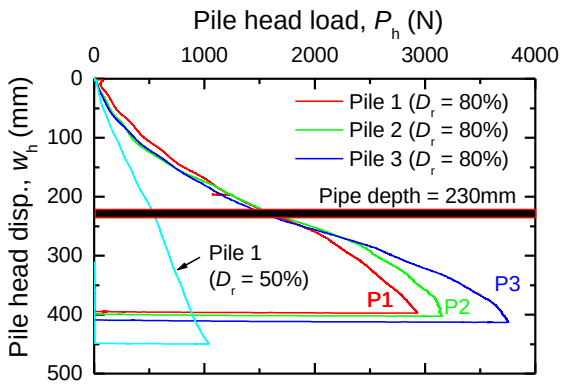

Fig. 8 Penetration resistance of pile in the dense and loose grounds

It is interesting notice that the ratio of CPT values between the dense and loose model was around 5 as shown in **Fig. 4**, while the ratios of the press-in force between them are less than 3 as indicated in **Fig. 8**. This is because the CPT values are related only with the resistance on the tip while the press-in force is related with both the resistance on the tip and on the shaft.

3.2. Behaviours of the buried pipe in the dense ground

Fig. 9 shows the bending moments of the buried pipe in the vertical direction, M_v, measured during installations of P1, P2 and P3 in the dense ground at various w_h. Bending moment, M_v, which causes curvature of the buried pipe convex downward is taken as positive. **Fig. 10** shows the bending moments of the buried pipe in the horizontal direction, M_h. Bending moment, M_h, which causes curvature of the buried pipe convex outward from the pile position is taken as positive.

Let us focus on **Fig. 9(a)** first. It is clearly seen that large bending moments are generated at the position of P1 (at x = 350 mm).

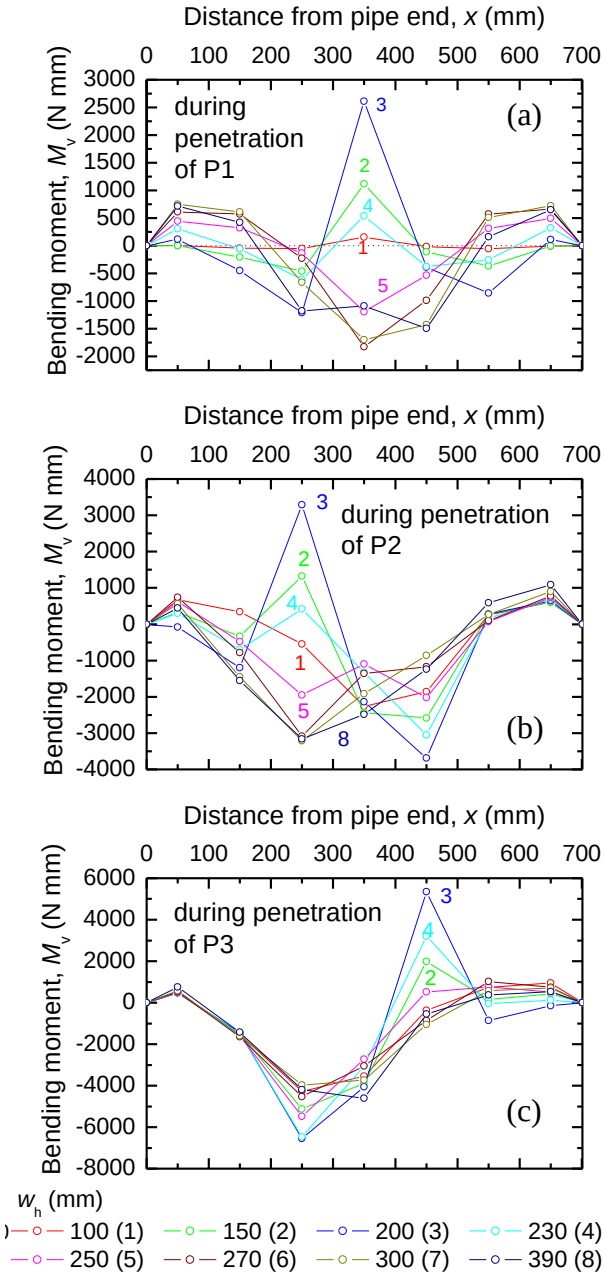

Fig. 9 Bending moments of the buried pipe in the vertical direction, M_v (in dense ground)

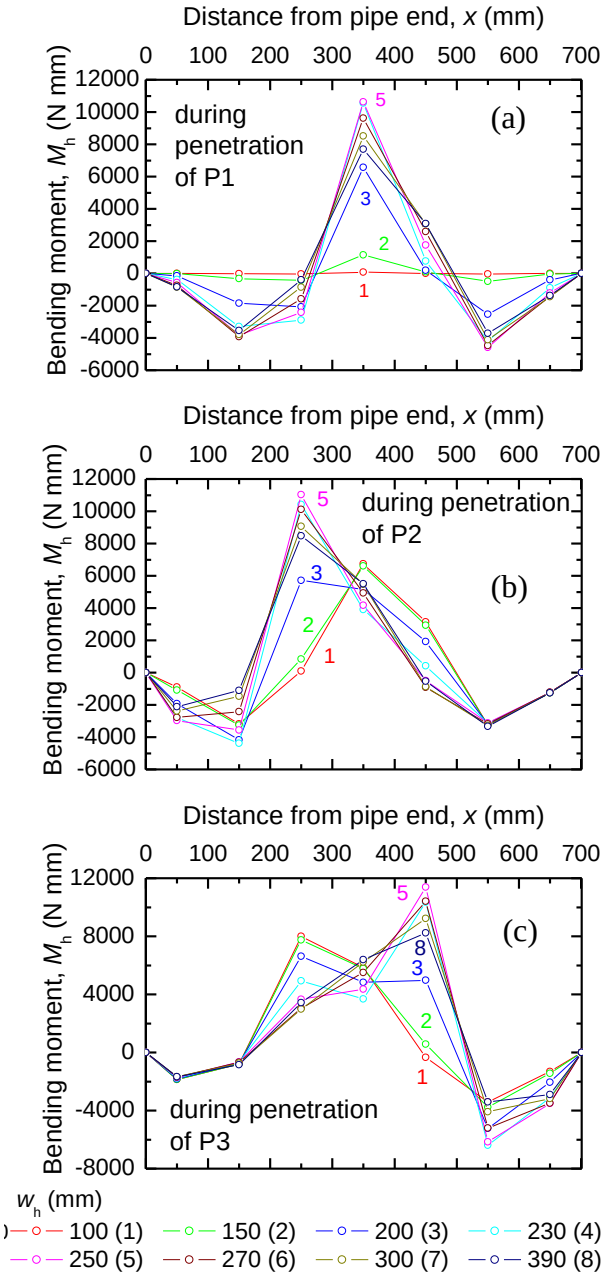

Fig.10 Bending moments of the buried pipe in the horizontal direction, M_h (in dense ground)

Change of distributions of M_v is complicated. M_v at x = 350 mm increases with increasing w_h until w_h increases to 200 mm. However, M_v decreases for further pile penetration, e.g. M_v at w_h = 230 mm (4) is smaller than that at w_h = 150 mm (2) and w_h = 200 mm (3). The peak M_v is caused at w_h = 200 mm, just before the pile tip level reach the depth of the buried PVC pipe (230 mm depth from the ground surface).

Next, let us look at **Fig. 10(a)** where bending moments in the horizontal direction, M_h, generated during the installation of P1 are shown. Large bending moments are generated at the position of P1 (at x = 350 mm). M_h at x = 350 mm increases with increasing w_h until w_h increases to 250 mm which a little bit deeper than the depth of the PVC pipe (230 mm depth from the ground surface). Thereafter, M_h starts to decrease a little bit for further pile penetration.

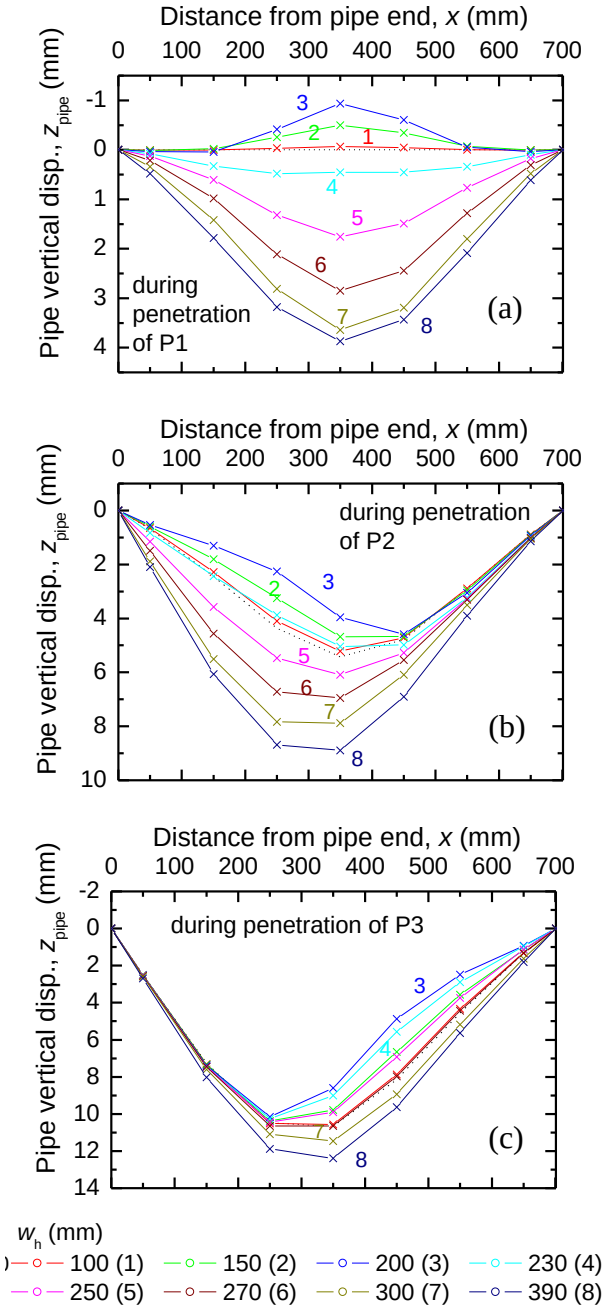

Fig. 11 Displacements of the buried pipe in the vertical direction, z_{pipe} (in dense ground)

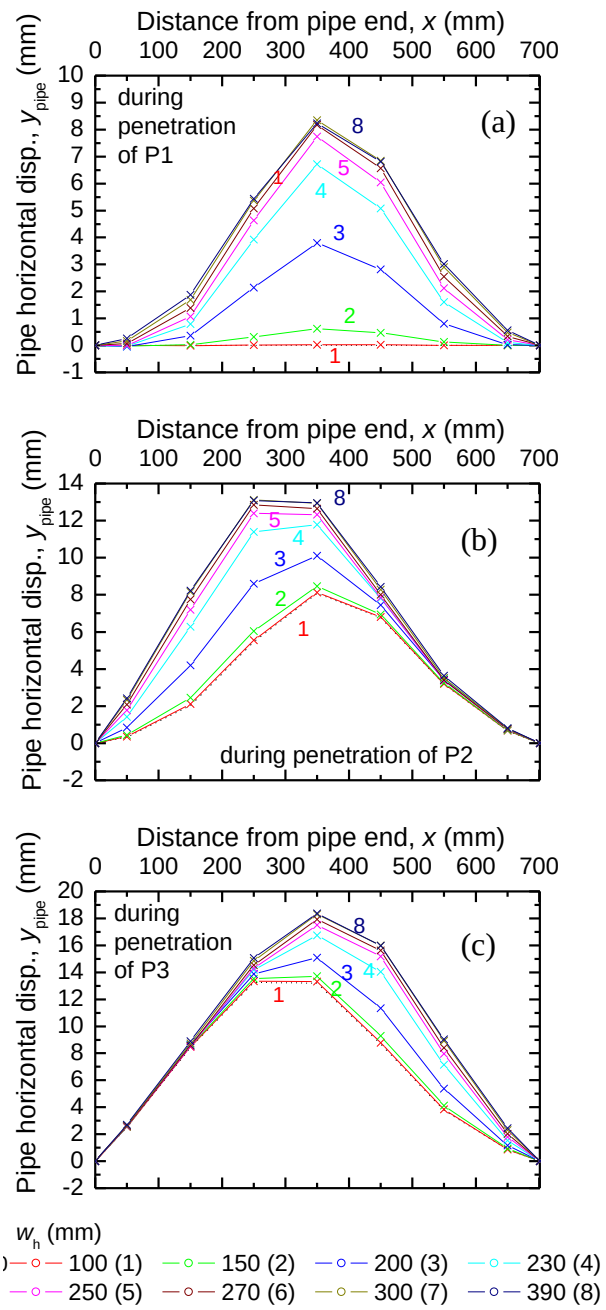

Fig. 12 Displacements of the buried pipe in the horizontal direction, y_{pipe} (in dense ground)

When P2 or P3 was installed, similar behaviours of bending moments, M_v and M_h, of the PVC pipe were observed. Large values of M_v and M_h were generated at the positions of P2 (x = 240 mm) or P3 (x = 430 mm). Similar to the changes of the vertical bending moments M_v during the installation of P1, M_v increases with increasing w_h until w_h of P2 or P3 increases to 200 mm. However, M_v decreases for further pile penetration (see **Figs. 9(b) and 9(c)**).

The horizontal bending moments, M_h, increase with increasing w_h until w_h increases to 250 mm. Thereafter, M_h starts to decrease a little bit for further pile penetration (see **Figs. 10(b) and 10(c)**).

The vertical displacement, z_{pipe}, and horizontal displacement, y_{pipe}, of the buried pipe were estimated from the measured distributions of M_v and M_h, respectively.

The vertical displacement of the pipe, z_{pipe}, was calculated using the elastic beam theory given by Eqs. (1) and (2).

$$M_v(x) = -EI\frac{d^2 z_{pipe}(x)}{dx^2} \quad (1)$$

$$z_{pipe}(x) = -\iint \frac{M_v}{EI}dxdx + C_1 x + C_2 \quad (2)$$

Two assumptions were made to obtain the distribution of z_{pipe}: 1) bending moments at both ends of the pipe are zero, and 2) displacements at the both ends of the pipe are zero. Similar procedure was used to estimate y_{pipe}.

Fig. 11 shows the displacements of the buried pipe in the vertical direction, z_{pipe}, during installations of P1, P2 and P3 in the dense ground at various w_h. Downward-displacement is taken as positive and upward-displacement is taken as negative. **Fig. 12** shows the displacements of the buried pipe in the horizontal direction, y_{pipe}. Horizontal displacement outward from the pile position is taken as positive.

Let us look at **Fig. 11(a)**. Large amplitudes of the vertical displacements are found at the position of P1 (x = 350 mm). Upward displacements of the buried pipe are caused until the pile tip depth, w_h, reaches 200 mm. When the pile tip depth reaches 230 mm which is the depth of the buried pipe, downward-displacements of the buried pipe are caused. Downward-displacements continue to increase until w_h reaches 300 mm. For further pile penetration, influence of the pile penetration on the vertical displacements is small.

It is seen from **Figs. 11(b) and 11(c)** that upward-displacements of the buried pipe are caused until w_h reaches 200 mm and downward-displacements are caused for further pile penetration. It is interesting that at the end of penetration of P3, the distribution of the vertical displacements of the buried pipe is almost symmetrical.

Next, let us see **Fig. 12(a)**. Horizontal displacements of the buried pipe, y_{pipe}, increase with increasing pile tip depth, w_h. Most part of the horizontal displacements occurs until w_h reaches 250 mm. The horizontal displacements of the buried pipe are scarcely affected by further pile penetration greater than w_h = 250 mm. It is seen from Fig. 12(c) that the distribution of the horizontal displacements of the buried pipe is almost symmetrical at the end of penetration of P3. The magnitudes of the horizontal displacements are about 1.5 times those of the vertical displacements.

3.3. Behaviours of the buried pipe in the loose ground

Measured behaviours of the buried pipe during penetration of P1 in the loose sand ground are shown in **Figs. 13 to 16**.

As mentioned earlier, the horizontal distance between the buried pipe and P1 was 85 mm, which was greater than 64 mm in the case of the dense ground.

Trends of the behaviours of the buried pipe in the loose ground are similar to those in the dense ground (**Figs. 9(a), 10(a), 11(a) and 12(b)**).

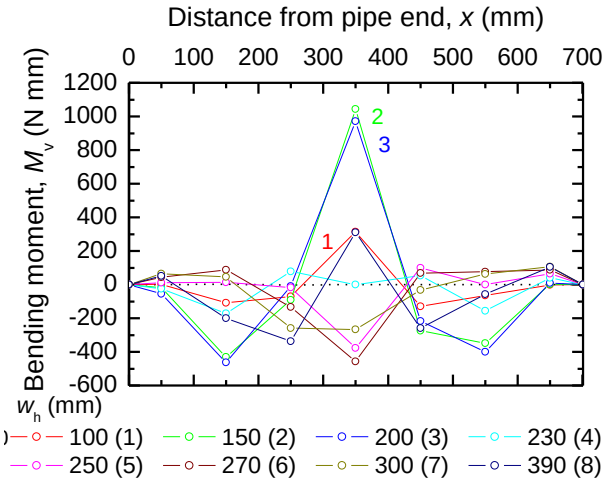

Fig. 13 Bending moments of the buried pipe in the vertical direction, M_v (in loose ground)

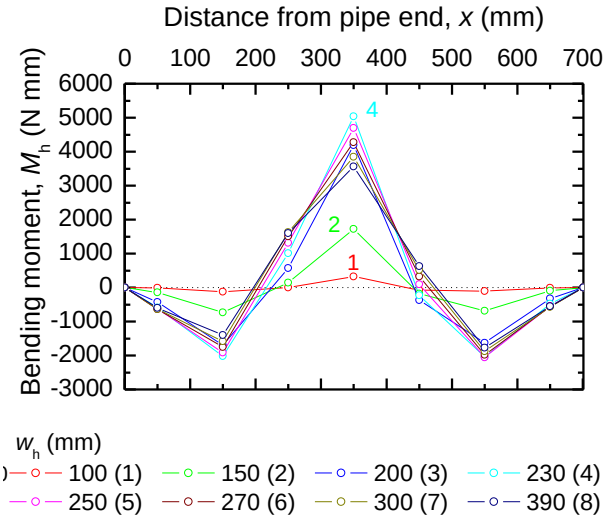

Fig.14 Bending moments of the buried pipe in the horizontal direction, M_h (in loose ground)

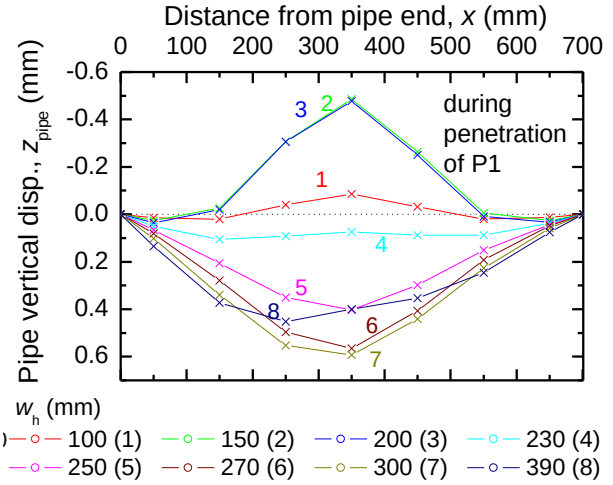

Fig. 15 Displacements of the buried pipe in the vertical direction, z_{pipe} (in loose ground)

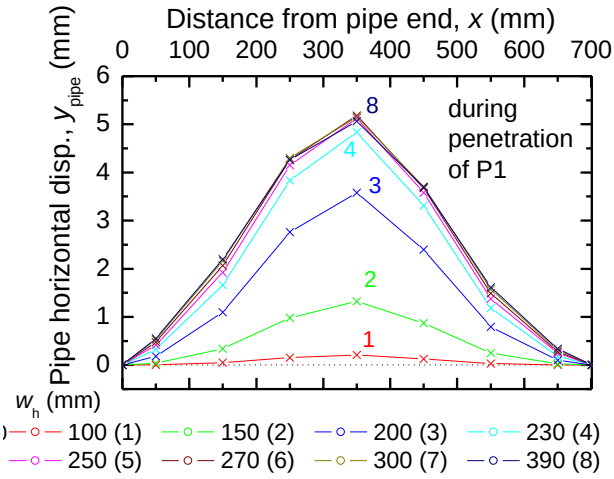

Fig. 16 Displacements of the buried pipe in the horizontal, y_{pipe} (in loose ground)

From comparison of **Figs. 15 and 16** with **Figs. 11(a) and 12(a)**, interesting findings are as follows. Magnitudes of displacements of the buried pipe in the vertical direction, z_{pipe} , in the loose ground are significantly smaller than those in the dense ground. For an example, the maximum downward displacement of the buried pipe is 0.6 mm in the loose ground, while that in the dense ground attains to 4 mm. In the case of the loose ground, magnitudes of the upward displacements and the downward displacements of the pipe are almost similar, while larger magnitudes of the downward displacements are generated in the dense ground.

Magnitudes of the horizontal displacements of the buried pipe in the loose ground are comparable to those in the dense ground.

4. Concluding remarks

Fundamental experiments were carried out to investigate the influence of newly installed piles on an existing buried pipe in dry sand. Although experimental conditions considered in this paper are limited, it is suggested from the experimental results that relative density of the sand, the distance between the installed piles and the buried pipe, the number of the newly installed piles are influential factors.

Although the fixity conditions of the buried pipe also may not be practical, the experimental method presented in this paper will be useful to investigate the the influence of newly installed piles on an existing buried pipe.

Acknowledgements

The authors would like to thank Mr. Shinya Shimono for his supports in the preparation and execution of the experiments in this research.

References

Vu, A. T. 2017. Experimental and Numerical Study on Behaviours of Pile Group and Piled Raft Foundations Having Batter Piles Subjected to Combination of Vertical and Cyclic Horizontal Loading, Dr. Thesis of Kanazawa University, 164pp.